Hindawi
Journal of Nanomaterials
Volume 2023, Article ID 3317584, 14 pages
https://doi.org/10.1155/2023/3317584

Research Article

Optimizing Numerous Influencing Parameters of Nano-SiO_2/Banana Fiber-Reinforced Hybrid Composites using Taguchi and ANN Approach

L. Natrayan,[1] **Raviteja Surakasi**,[2] **Pravin P. Patil**,[3] **S. Kaliappan**,[4] **V. Selvam**,[5] **and P. Murugan**[6]

[1]*Department of Mechanical Engineering, Saveetha School of Engineering, SIMATS, Chennai 602105, Tamil Nadu, India*
[2]*Department of Mechanical Engineering, Lendi Institute of Engineering and Technology, Jonnada, Vizianagaram 535005, Andhra Pradesh, India*
[3]*Department of Mechanical Engineering, Graphic Era Deemed to be University, Bell Road, Clement Town, Dehradun 248002, Uttarakhand, India*
[4]*Department of Mechanical Engineering, Velammal Institute of Technology, Chennai 601204, Tamil Nadu, India*
[5]*Department of Mechanical Engineering, Kongunadu College of Engineering and Technology, Trichy 621215, Tamil Nadu, India*
[6]*Department of Mechanical Engineering, Jimma Institute of Technology, Jimma University, Jimma, Ethiopia*

Correspondence should be addressed to P. Murugan; murugan.ponnusamy@ju.edu.et

Received 12 August 2022; Revised 4 December 2022; Accepted 5 April 2023; Published 27 April 2023

Academic Editor: R. Lakshmipathy

High specific strength, strength-to-weight ratio, cheap cost, and other advantages, nanofillers are now the subject of most research on natural fibers. The current research's main goal is to combine the Taguchi and artificial neural networks (ANN) approaches to maximize the mechanical characteristics of nanocomposites. The parameters: (i) nano-SiO_2 wt%, (ii) banana fiber wt%, (iii) compression pressure in MPa, and (iv) compression molding temperature in °C were selected to achieve the objectives above. An L_{16} orthogonal array was used to optimize the process parameters based on the Taguchi technique. According to the intended experiment, mechanical characteristics, such as tension, bending, and impact strength, were assessed. The ANN was used to forecast outcomes that were optimized. The fiber mat thickness of banana fiber and the weight ratio of nano-SiO_2 showed a considerable improvement in the mechanical characteristics of hybrid composites. According to the Taguchi technique, the most significant mechanical characteristics were 47.36 MPa tensile, 64.48 MPa flexural, and 35.33 kJ of impact under circumstances of 5% SiO_2, 19 MPa pressure, and 110 °C. With 95% accuracy, ANN-predicted mechanical strength. The ANN forecast was more accurate than the regression model and experimental data. The above nanobased hybrid composites are mainly employed to satisfy the needs of the contemporary vehicle sector.

1. Introduction

Due to the overuse of plastic materials, which results in numerous pollution problems and health problems for all living things, the entire world is at risk. Utilizing bio-based natural materials like jute, hemp, wheat, pineapple, banana, coco fiber, wool, ramie, and roselle can significantly minimize this [1, 2]. The concentration of lignocellulosic biomass, hemicellulose, and lignin determines the qualities of natural fibers, which vary depending on the production region. These fiber combinations are utilized for various purposes, such as packing, thermos insulators, vibration-dampening materials, and building materials [3, 4]. It demonstrated lower mechanical properties than synthetic fibers like fiberglass, graphene, glass, and obsidian. The mechanical performance of polymeric materials is increased by the hybridization of natural and synthetic fibers [5, 6]. Hybridization enhanced the composite's characteristics because it increased their interfacial adherence. Owing to their water-absorbing nature, such natural fabrics have inferior characteristics, which results in poor adherence when using hydrophilic polymers [7]. The addition

of up to 35% fiber improved the mechanical properties of the pineapple/flax-based composite materials significantly [8]. That compressed molding technique offered a compressive pressure of 14 MPa and a temperature of 120°C. At a wt% of 30%, sisal/pineapple epoxy matrix composites showed good tension, bending, and shock characteristics. Ribbed and simple type weave designs were utilized to manufacture banana/kenaf polymer composites using the hand lay-up method [9, 10]. A simple type arrangement was used to display the ultimate compressive characteristics.

In addition to mechanical qualities, thermodynamic and morphological durability, flame and chemical resistance, photoelectrochemical characteristics, and other characteristics, polymer nanocomposites constitute a novel class of composites [11]. Due to their unique qualities and multiple uses in advanced technologies, nanocomposites containing mineral fillers have garnered considerable interest [12]. Inorganic nanoparticles and polymeric matrices are mainly combined to provide the qualities of polymeric composites. Due to their high thermal properties, environmental resilience (durability), electrical, toxicological, and mechanical behavior, conductive polymers can be used as a nanocomposite matrix [13, 14]. Specific polymers like epoxy matrix are widely recognized as highly fragile. Due to this drawback, such polymers can only be used in goods with great shock and breakage resistance. The polymer nanocomposites' mechanical properties were enhanced by adding fillers to the matrix material [15]. Nanofillers contain a lot of surface area, which makes them chemically active and facilitates easier matrix interaction. To lower production costs, address some of the drawbacks of polymers, and broaden their uses, stiff fillers can strengthen polymeric materials in various ways. The type of the polymers and the filler's fraction determines whether additives affect such polymers' properties [16, 17]. Several aspects of polymers, including their mechanical, thermodynamic, electromagnetic, and physical properties, can be changed by fillers. To create polymer materials and comprehend their behavior, it is crucial to have the proper weight, chemical composition, semicrystallinity, chemical solubility, and heat resistance of the polymer as well as the surface energy, chemical composition, and dispersion of the nanoparticle [18, 19]. Alternate polymerization reactions, in vivo polymerization processes, direct mixing, solution dispersal, the sol–gel technique, melt compounding, melt extruding, and injection molding are all methods for producing thermoplastic matrix composites [20, 21]. Although each method is unique, the ultimate morphologies of the nanocomposites are crucial. The thermoplastic interaction that supports effective dispersal and dispersion of the nanoparticles in the polymer matrices also has a role in determining the shape. Due to the substantial surface area between the polymer matrices and nanofillers, composite materials offer better physical and mechanical characteristics than host polymers [22, 23].

A model based on recently observed measurements must be created to forecast material quality. This might drastically reduce the additional experimental labor needed to create lightweight structures. For this aim, artificial neural networks (ANN) have recently been created in this discipline. ANN employs linked nodes (known as neurons), in which the connections are "evaluated" to simulate the functionality of a human brain [24, 25]. The biological nervous system inspired ANN. Such a network is capable of learning from mistakes and figuring out how to solve functional relationships that are rather complicated, convoluted, and multifunctional [26, 27]. Since there are no prescribed rules concerning the nature of the issue, the network defining the connection is created immediately by instances of this methodology, which distinguishes it from traditional processes. The neural network can independently establish the relationship between causes (input data) and effects (output data) throughout development [28, 29]. ANN has also been demonstrated to be an effective analytical tool for solving issues in various material science and technology fields [30, 31].

As the literature shows, selecting the proper mechanical properties parameters for nanocomposites related to natural fibers is problematic. This may be resolved by utilizing the Taguchi-based technique, which aids in determining the optimal multiresponse outcomes for bending, shock, and tension characteristics.

Table 1: Parameters and their constraints.

Sl. no.	Constraints	Symbols	Stages			
			S1	S2	S3	S4
1	Nano-SiO_2 (wt%)	A	0	2.5	5	7.5
2	Banana fiber mat (gsm)	B	150	200	250	300
3	Molding pressure (MPa)	C	10	13	16	19
4	Molding temperature (°C)	D	100	110	120	130

2. Experimental Works

2.1. Materials. Organic banana fibers from the GVR Enterprises in Madurai, India, were employed as a reinforcing material. As the matrix material, epoxy grade LY556, with lower density, excellent corrosion resistance, superior mechanical performance, and specific stiffness, was combined with curing agent HY951. The nano-SiO_2 particles are supplied by Naga Chemical Industries in Chennai, Tamil Nadu, India. In Table 1, the composition and characteristics of fiber reinforcements are described. Photographic image of banana fiber, and nano-SiO_2, epoxy matrix materials are shown in Figure 1(a)–1(c), respectively.

The banana fibers were extracted in the following manner. The inside peel of a banana plant is used to harvest the banana fiber. The banana stem is physically skinned in the apparatus used to harvest banana fibers. The outer peel, which has been removed and is dark and greenish, is wasted. The stem now has a white-colored snarl. The banana fiber is extracted from this stem bark. Its interior layer, which has been removed, is handled via a machine with compression crushers and a mechanism for sorting fibers. Because the white inner bark has a significant quantity of humidity inside of it, the peel must be free of such humidity. Compression rollers aid in reducing the moisture content of fibers. The white peel is removed and run through the rollers nipped to remove moisture. Humidity purges like a sugarcane juice press. The peeling stem is fed as long as possible between

Figure 1: Photographic image of (a) banana fiber; (b) nano-SiO_2; (c) epoxy matrix materials.

the roller nip by the machine operator while holding one end of a peeling stump.

2.2. Fabrication of Hybrid Composites. To improve the fibers' crystalline nature and compliance with the matrix composites, the exterior of the fibers was treated with 5% NaOH to eliminate waste materials, wax components, certain hemicellulose, and lignin. The alkali-treated fibers underwent a thorough cleaning, were dried in a warm environment, and were then roasted in an oven at 70°C for 3 hr. The epoxy resin was thoroughly mixed with different weight proportions of nanofillers using a glass steel rod. The mixing process was then repeated with a mechanical stirrer at 30 RPM. In the end, a 10 : 1 proportion of epoxy resin and hardener was applied to the nanomixture. Banana fiber reinforcement ranging from 150 to 300 gsm-based thick fiber mat was inserted in a steel mold to perform compression molding ($150\times 150\times 3\ \text{mm}^3$). The desired material in wt% is poured into the mold with reinforcing fibers at temperatures and pressures ranging from 10 to 19 MPa and 100 to 130°C. The following section provides further information on how Taguchi-based analysis was used throughout the procedure. Table 1 reveals the parameters and their levels used in the present research.

2.3. Taguchi Approach. The typical investigative plan continues to be overly complicated and impractical because it calls for several investigations. Fewer experiments are used in the Taguchi approach. The effects of process factors on mechanical qualities are shown by S/N ratio and analysis of variance (ANOVA). The Taguchi approach to the experimental process is a helpful procedure to rationally explain, investigate, and optimize various process elements to get the intended outcome. Using this method, the primary restrictions are identified by converting the outcome of the investigation into an S/N proportion. According to the compelling argument for improving the critical feature, the S/N ratio features were divided into three categories: (i) more excellent was best, (ii) nominally better, and (iii) smallest was best. Irrespective of the performance characteristic set, the performance characteristic is larger than the S/N ratio. Therefore, the level with the highest S/N ratio is the best level for the variable [17]. The composites' flexural, tensile, and impact strengths were evaluated throughout the testing process, utilizing the more excellent principle. Since more excellent is better, S/N ratios of prominent qualities are written as follows:

$$\text{S/N ratio} = -10\log_{10}\frac{1}{e}\sum_{a=i}^{e}\frac{1}{X_{ab}^2}. \quad (1)$$

2.4. Mechanical Characterization. The samples underwent mechanical testing following ASTM requirements following the compression molding process. The ASTM D 638-03 protocol was used to perform tensile testing on a universal testing machine with the highest capability of 15,000 kgf. Following the ASTM D 790 protocol, Flexural testing was conducted on the same universal testing machine. Following the ASTM D 256 standard, an Izod impact tester was utilized for hardness tests. To verify the measurements, every outcome was examined again.

3. Result and Discussion

3.1. S/N Ratio Indications. To examine the process improvements and to choose defect-free, max strength nanocomposite from a wide variety of system variables, mechanical characteristics for the L16 OA were evaluated. In this study, the distinctive feature of observed tension, bending, and impacts depend on selected features. The statistics for the tests conducted in the Taguchi experimental L16 factorial design were done using Minitab 17 software. Following the "Bigger is Better" choice, the S/N ratio determined the mechanical qualities. The best hybrid composite factors have the highest S/N ratios [32]. L16 OA and S/N ratios for mechanical characteristics are shown in Table 2. The reaction rate mean was determined for each of the 16 experiment conditions. The effect and ideal situation for the elements under consideration were determined via ANOVA and S/N ratio. S/N ratio did the most fantastic job of condensing the diversity in excellent qualities. For this investigation, larger-the-better was taken into account [33, 34].

The effect plot (bigger is better) on the S/N ratio for mechanical characteristics is shown in Figure 2(a)–2(c).

Table 2: Experimental design and their outcomes.

Run	A	B	C	D	Tensile	Flexural	Impact	S/N of tensile	S/N of flexural	S/N of impact
1	0	150	10	100	26.57	49.15	18.56	27.81	33.83	25.37
2	0	200	13	110	33.24	57.82	28.67	29.89	35.24	29.15
3	0	250	16	120	35.24	55.62	26.47	30.94	34.90	28.46
4	0	300	19	130	34.9	56.48	27.33	30.60	35.04	28.73
5	2.5	150	13	120	33.57	55.15	26	30.26	34.83	28.30
6	2.5	200	10	130	31.88	58.46	29.31	31.10	35.34	29.34
7	2.5	250	19	100	40.57	63.15	34	32.16	36.01	30.63
8	2.5	300	16	110	41.9	64.48	35.33	32.44	36.19	30.96
9	5	150	16	130	33.9	56.48	27.33	30.60	35.04	28.73
10	5	200	19	120	38.25	60.83	31.68	31.65	35.68	30.02
11	5	250	10	110	41.87	64.45	35.3	32.44	36.18	30.96
12	5	300	13	100	47.36	60.32	31.17	33.51	35.61	29.87
13	7.5	150	19	110	35.46	58.04	28.89	30.99	35.27	29.21
14	7.5	200	16	100	36.98	59.56	30.41	31.36	35.50	29.66
15	7.5	250	13	130	37.97	60.55	31.4	31.59	35.64	29.94
16	7.5	300	10	120	38.12	60.7	29.56	31.62	35.66	29.41

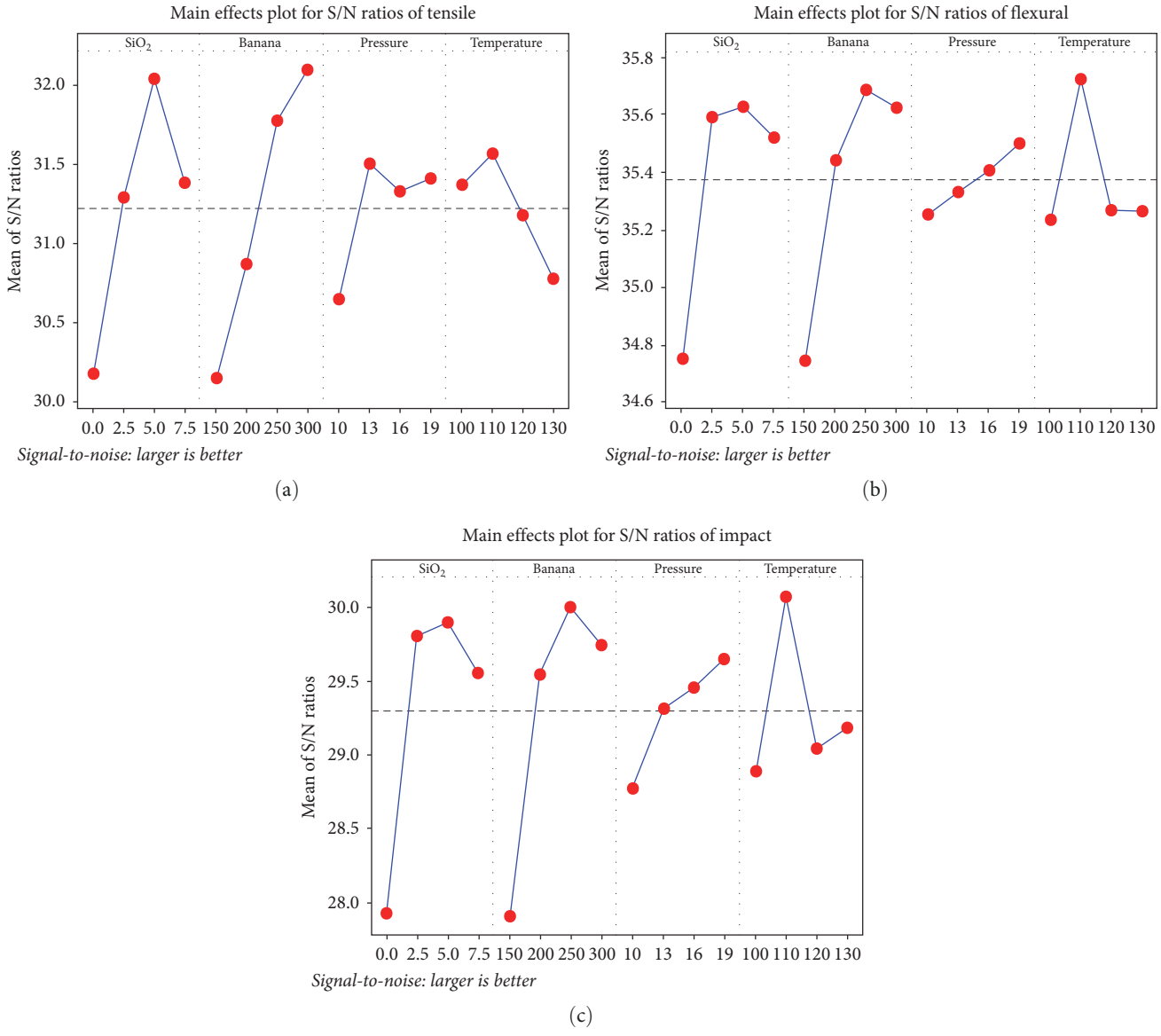

Figure 2: S/N ratio larger the better plot for (a) tensile; (b) flexural; (c) impact strength of nanocomposites.

Table 3: S/N ratio of tensile behavior.

Levels	SiO_2 nanopowder (wt%)	Woven banana type (gsm)	Molding pressure (MPa)	Molding temperature (°C)
1	30.18	30.15	30.65	31.38
2	31.30	30.88	31.51	31.58
3	32.05	31.78	31.34	31.18
4	31.39	32.11	31.42	30.78
Delta	1.87	1.96	0.86	0.80
Rank	2	1	3	4

Table 4: S/N ratio of flexural behavior.

Levels	SiO_2 nanopowder (wt%)	Woven banana type (gsm)	Molding pressure (MPa)	Molding temperature (°C)
1	34.75	34.74	35.25	35.24
2	35.59	35.44	35.33	35.72
3	35.63	35.68	35.41	35.27
4	35.52	35.62	35.50	35.26
Delta	0.87	0.94	0.25	0.49
Rank	2	1	4	3

Table 5: S/N ratio of impact strength.

Levels	SiO_2 nanopowder (wt%)	Woven banana type (gsm)	Molding pressure (MPa)	Molding temperature (°C)
1	27.93	27.90	28.77	28.88
2	29.81	29.54	29.32	30.07
3	29.89	29.99	29.45	29.05
4	29.56	29.75	29.65	29.19
Delta	1.97	2.09	0.88	1.19
Rank	2	1	4	3

Table 6: ANOVA for tensile behavior.

Source	DF	Seq SS	Contribution	Adj SS	Adj MS	*F*-value	*P*-value
SiO_2	3	125.166	35.68	125.166	41.722	32.43	0.009
Banana	3	164.69	46.94	164.690	54.897	42.67	0.006
Pressure	3	26.368	7.52	26.368	8.789	6.83	0.074
Temp	3	30.754	8.77	30.754	10.251	7.97	0.061
Error	3	3.860	1.10	3.860	1.287		
Total	15	350.838	100				

The ideal conditions for all mechanical qualities were 5 wt% SiO_2, 300 gsm of banana fiber mat, 19 MPa pressure, and 110°C molding temperature. The larger and better S/N reaction exhibited the most excellent mechanical properties. Tables 3–5 display the effects of the control variable on the tension, bending, and impact properties with the S/N ratio reaction.

3.2. Analysis of Variance. To evaluate the importance of discontinuous functional units, an ANOVA was performed. The process parameter known as *F*-test is what is thought to have an influence on the tension, bending, and impact characteristics. The proportion of contributions for every processing parameter is shown in Tables 6–8 under Column F. The contribution % for each element is shown in Figure 3. The contributing proportion is the portion of the trial's overall difference that took every significant effect into account [35, 36].

The percentage contribution of the process variables on mechanical behavior is shown in Figure 3(a)–3(c). To reach the maximum tension, Table 6's *F*-value and contributing % function as controlled variables. The *p*-value specifies the likelihood of recurring factors. Banana fiber mat has contributions from nano-SiO_2 of 35.68%, 46.94%, pressure, and temperature of 7.52%, and 8.77%, respectively. Thus, it is

Table 7: ANOVA for flexural behavior.

Source	DF	Seq SS	Contribution	Adj SS	Adj MS	*F*-value	*P*-value
SiO_2	3	89.317	39.56	89.317	29.772	21.65	0.016
Banana	3	87.458	43.17	97.458	32.468	23.62	0.014
Pressure	3	4.882	2.16	4.882	1.627	1.18	0.447
Temp	3	29.971	13.28	29.971	9.990	7.27	0.069
Error	3	4.125	1.83	4.125	1.1375		
Total	15	225.752	100				

Table 8: ANOVA for impact strength.

Source	DF	Seq SS	Contribution	Adj SS	Adj MS	*F*-value	*P*-value
SiO_2	3	98.260	39.07	98.260	32.753	42.93	0.006
Banana	3	103.467	41.14	103.467	34.48	45.21	0.005
Pressure	3	11.461	4.56	11.461	3.820	5.01	0.109
Temp	3	35.992	14.31	35.992	11.997	15.73	0.024
Error	3	2.289	0.91	2.289	0.762		
Total	15	251.47	100				

abundantly evident that banana fiber mat is the main factor in achieving excellent mechanical properties. According to Table 6, banana fiber mat plays a significant role in achieving flexural strength; it provided 43.17% and 39.56% of the nano-SiO_2, respectively, with pressure and temperature coming in second and third place with 2.16% and 13.28%. Banana fiber mat gives 41.14% impact strength, followed by nano-SiO_2, which contributes 39.07%, molding pressure, which contributes 4.56%, and temperature, which provides 14.31%. The findings indicate that the banana fiber mat and nano-SiO_2 are the main factors in the current study's achievement of the most significant mechanical strength properties.

3.3. Regression Equation. The regression equation model was established using four control conditions and the four levels considered for this investigation. By lowering the sum of the squared royalties, the traditional regression approach was utilized to create the formulas for tension, bending, and impact. The resulting regression models are as follows:

$$\begin{aligned}\text{Tensile} = {} & 36.736 - 4.249\,S1 + 0.244\,S2 + 3.609\,S3 \\ & + 0.396\,S4 - 4.361\,B1 - 1.649\,B2 + 2.176\,B3 \\ & + 3.834\,B4 - 2.126\,P1 + 1.299\,P2 + 0.269\,P3 \\ & + 0.559\,P4 + 1.134\,T1 + 1.381\,T2 \\ & - 0.441\,T3 - 2.074\,T4,\end{aligned} \tag{2}$$

$$\begin{aligned}\text{Flexural} = {} & 58.827 - 4.060\,S1 + 1.482\,S2 + 1.692\,S3 \\ & + 0.885\,S4 - 4.123\,B1 + 0.340\,B2 + 2.115\,B3 \\ & + 1.668\,B4 - 0.638\,P1 - 0.367\,P2 + 0.207\,P3 \\ & + 0.798\,P4 - 0.798\,T1 + 2.370\,T2 \\ & - 0.753\,T3 - 0.835\,T4,\end{aligned} \tag{3}$$

$$\begin{aligned}\text{Impact} = {} & 29.463 - 4.206\,S1 + 1.697\,S2 + 1.907\,S3 \\ & + 0.602\,S4 - 4.268\,B1 + 0.554\,B2 + 2.329\,B3 \\ & + 1.384\,B4 - 1.281\,P1 - 0.153\,P2 + 0.422\,P3 \\ & + 1.012\,P4 - 0.928\,T1 + 2.584\,T2 \\ & - 1.036\,T3 - 0.621\,T4.\end{aligned} \tag{4}$$

The regression equation's variables that exhibit favorable indications cause the mechanical characteristics to be worth more, while those that generate negative indications for the mechanical properties to be worth less. The ideal conditions for all mechanical qualities were 5 wt% SiO_2, 300 gsm of banana fiber mat, 19 MPa pressure, and 110°C of molding temperature. The weight ratio of SiO_2 nanofiller boosted the strength of natural nanocomposites by up to 5%. When the weight ratio of the SiO_2 nanofiller was raised further, the matrix and reinforcement interaction deteriorated [37]. This is a result of the particle and resin being mixed improperly. The banana's gsm fiber has beneficial effects on all levels. It proves that stronger banana weave will increase nanocomposite strength. It is because the existence of heavier, high cellulose components reduces the effects of vacancies. The results of the tests also showed that mechanical properties decreased as the heating rate (130°C) rose. When the fiber was exposed to intense compressive pressure, it was easy to see how quickly its mechanical qualities degraded (19 MPa). This decline in mechanical properties may be due to the thermal deterioration of natural fibers (banana) at high temperatures [27]. The lowest strength may also come from poor matrix-fiber interface strength at low compressive pressures. An optimal pressure with increased strength was discovered at a pressure of 19 MPa, which may be regarded as the greatest pressure that can be used to increase mechanical properties without affecting the fiber structure, indicating that complete reinforcing occurs [38, 39]. The surface plot of mechanical characteristics with regard to different parameters is shown in Figure 4.

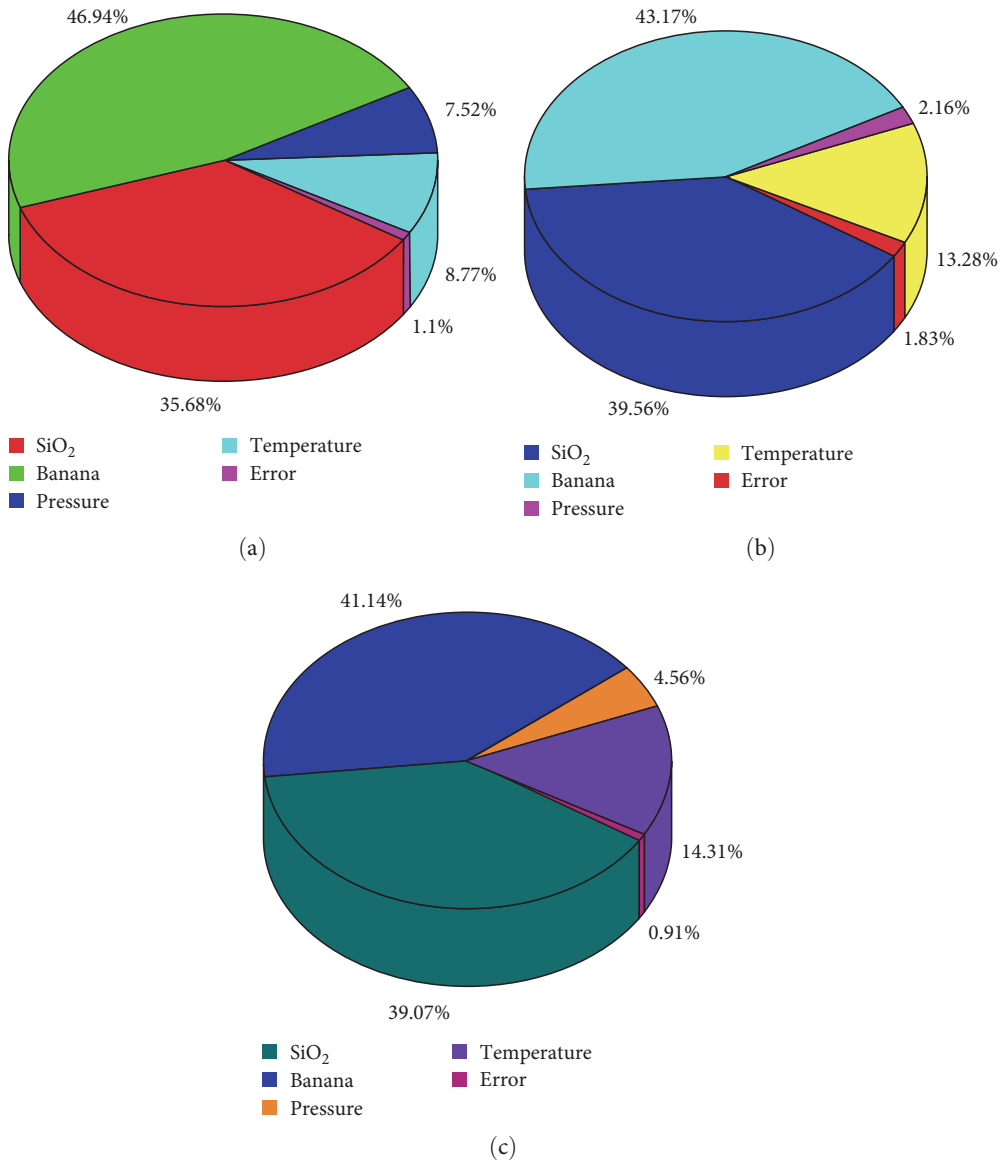

Figure 3: Nanocomposite parameter contributions (a) tensile; (b) flexural; (c) impact strength.

3.4. Artificial Neural Networks. To match and resolve the research data gathered through various methods, ANN are utilized. This model has three layers: inputs, outputs, and hiding. The output layer informs the operators, the hiding layer processes data, and the input layer is often used for data entry. The ANN technique is used to forecast the mechanical performance in MATLAB R2015. Figure 5 shows the ANN structure of the current research. Inputs included nano-SiO_2, banana fiber, molding pressure, and temperature; outputs were tensile, bending, and impact strength. A backpropagation using feed-forward for the prediction of mechanical characteristics was used. An ANN using a Levenberg–Marquardt training tool was also used. There are four neurons in each of the hidden layers. Three groups of input and output data are created using the ANN; these categories are training (60%), tests (20%), and verification (20%) [24].

Ten of the 16 measurements were selected for training, three for verification, and three for testing. The artificial neural toolkit received all of the input and output information. It serves as a stand-alone test for the networks. Four neurons are connected to four outcomes established in the output nodes, whereas one or two neurons are defined in the hidden state [40, 41]. Four neurons respond to input factors established in the input nodes. Specified input and output data sets were introduced into the 4-4-4-3 ANN design after constructing the networks. It is seen in Picture 5. The correlation analysis and the proportional confidence interval were used to evaluate the model. The comprehensive flow chart for the ANN prediction is shown in Figure 6. The developed ANN system calculates the % of expected error by using Equation (5).

$$\%\ \text{of predicted error} = \frac{\text{Experimental data} - \text{ANN data}}{\text{Experimental data}} \times 100. \tag{5}$$

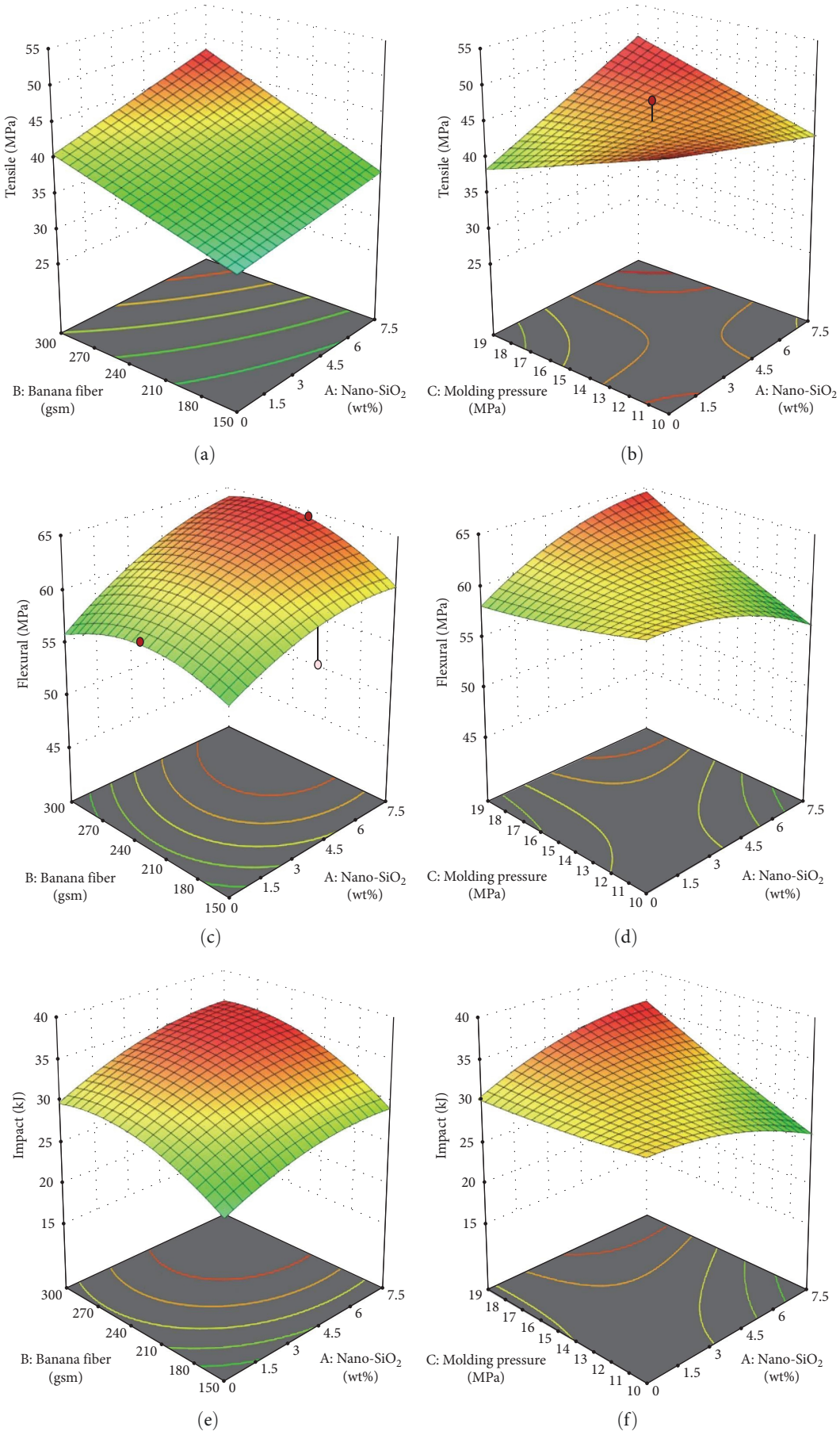

Figure 4: Surface plot of nanocomposites (a and b) tensile; (c and d) flexural; (e and f) impact strength.

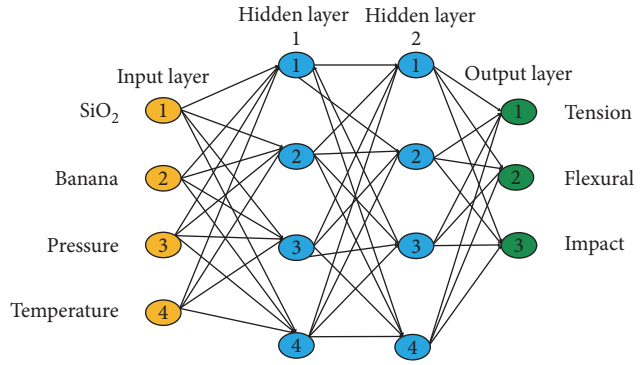

Figure 5: ANN structure of the current research.

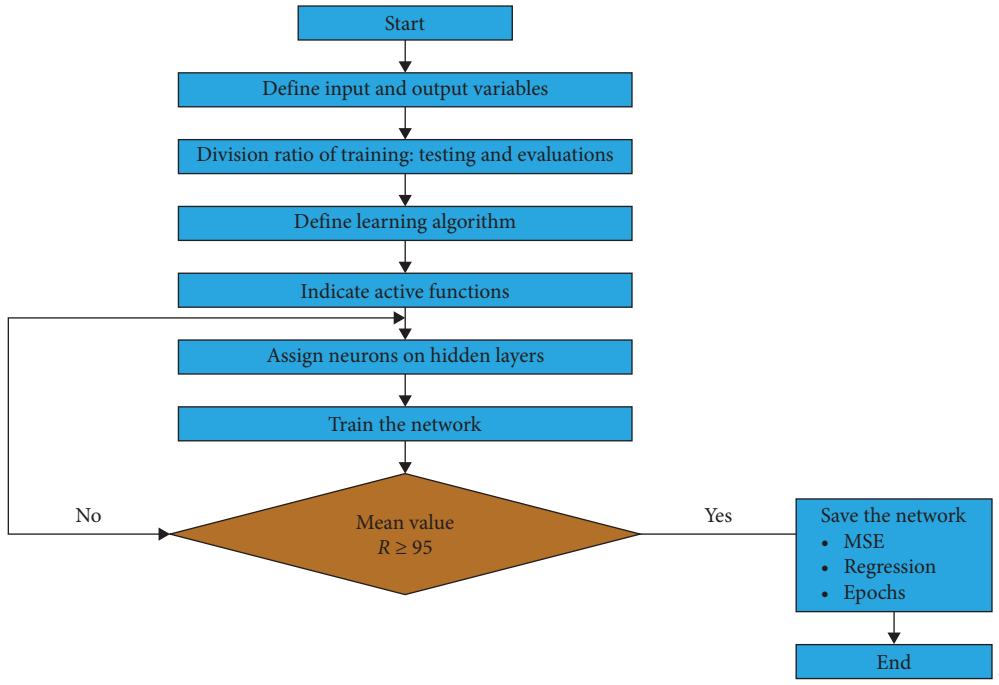

Figure 6: Prediction of ANN flowchart.

Table 9 displays the statistics' learning, verification, and assessment sets with the estimated error percentage. The average % of projected error (0.9232) was less than 3%, and the correlation for all categories was 0.9718 for tensile, 0.9567 for flexural, and 0.9620 for impact. Figure 7(a)–7(c) demonstrates the predictive accuracy of the ANN model 7(c). Figure 8(a)–8(c) illustrates the research observations with a significant link between network responsiveness. Experimental validation is done whenever the measured variables are within their ideal ranges. It is employed to assess the accuracy of the experimental findings.

The outcomes of experimental, predictive, and ANN are described in Figure 8. It has been determined that both the Taguchi and ANN approaches produce trustworthy findings based on the study of experimental data. In comparison to experimental values acquired by Taguchi, the findings of the ANN approach were higher, resulting in more excellent predictions with 95% reliability. The ANN optimum model aids in incorporating the process factors that result in the desired cast composites. Given that it saves money and time, this is ideal for natural fiber-based automobile sectors. Table 10 exhibits the optimum outcomes of mechanical properties based on the experimental, regression, and ANN results.

4. Conclusion

L16 OA was extensively used in experimental trials to evaluate the mechanical properties of the manufactured composites, such as tension, bending, and impact. The Taguchi technique's predicted optimal parameter for nano-SiO_2/banana-based hybrid composites were compared with ANN in this work. Hemp fiber mat in gsm, molding pressure, temperature, and nano-SiO_2 wt% were the four parameters and levels considered for this study. The following findings were drawn from

Table 9: Comparison of experimental vs. ANN results.

Sl. no.	Experimental results			ANN results			Predicted error		
	Tension	Flexural	Impact	Tension	Flexural	Impact	Tension	Flexural	Impact
1	26.57	49.15	18.56	27.25	49.52	19.09	−2.5734	−0.7426	−2.859
2	33.24	57.82	28.67	33.64	57.40	28.55	−1.1996	0.72639	0.40766
3	35.24	55.62	26.47	34.61	56.63	27.28	1.78419	−1.8114	−3.0719
4	34.9	56.48	27.33	34.93	56.69	27.34	−0.0752	−0.3674	−0.048
5	33.57	55.15	26	33.60	55.36	26.01	−0.0782	−0.3762	−0.0505
6	31.88	58.46	29.31	31.25	59.47	30.12	1.97224	−1.7234	−2.7742
7	40.57	63.15	34	40.97	62.73	33.88	−0.9829	0.66508	0.34375
8	41.9	64.48	35.33	42.58	64.85	35.86	−1.6319	−0.5661	−1.5019
9	33.9	56.48	27.33	34.30	56.06	27.21	−1.1763	0.74363	0.42764
10	38.25	60.83	31.68	39.01	61.20	32.21	−1.9869	−0.6	−1.675
11	41.87	64.45	35.3	42.21	64.66	35.31	−0.812	−0.322	−0.0372
12	47.36	60.32	31.17	46.98	61.33	31.98	0.80236	−1.6703	−2.6087
13	35.46	58.04	28.89	35.01	59.05	29.70	1.26904	−1.7359	−2.8146
14	36.98	59.56	30.41	37.01	59.77	30.42	−0.071	−0.3484	−0.0432
15	37.97	60.55	31.4	38.65	60.92	31.93	−1.8008	−0.6028	−1.6899
16	38.12	60.7	29.56	38.52	60.28	29.44	−1.046	0.69193	0.39538

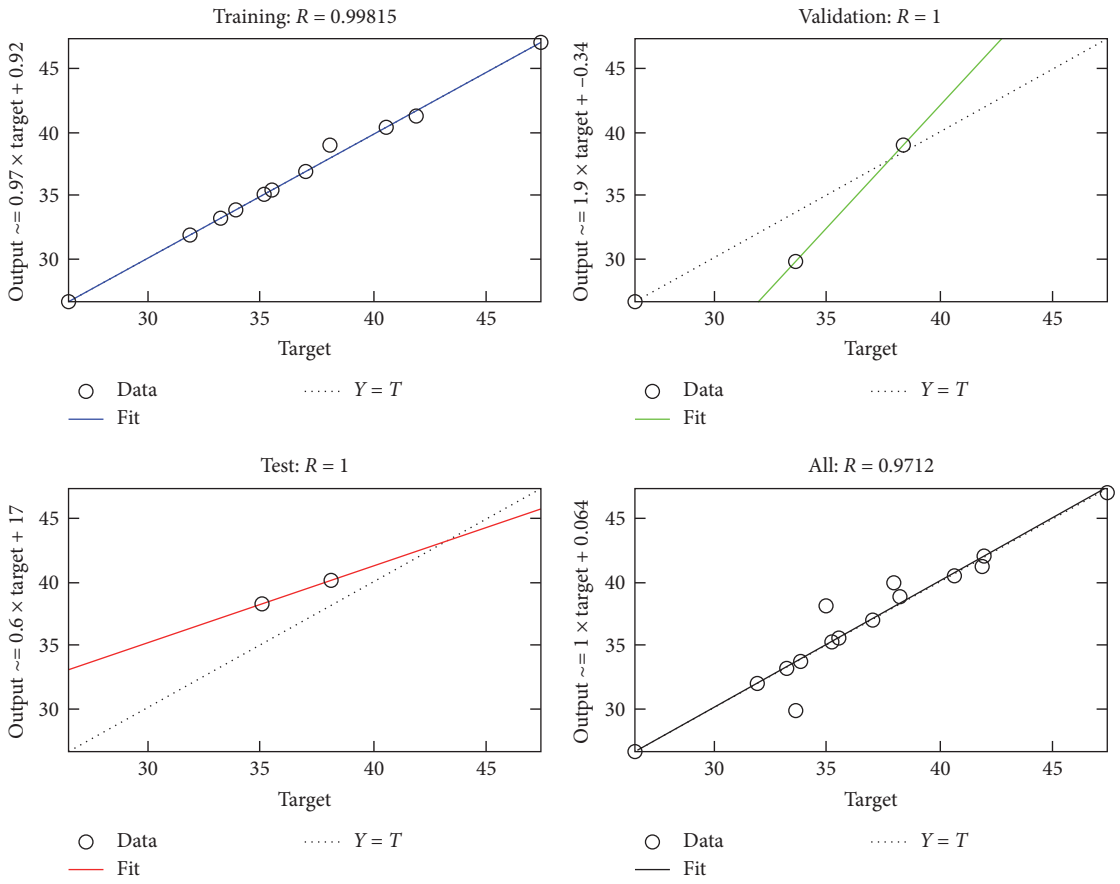

(a)

Figure 7: Continued.

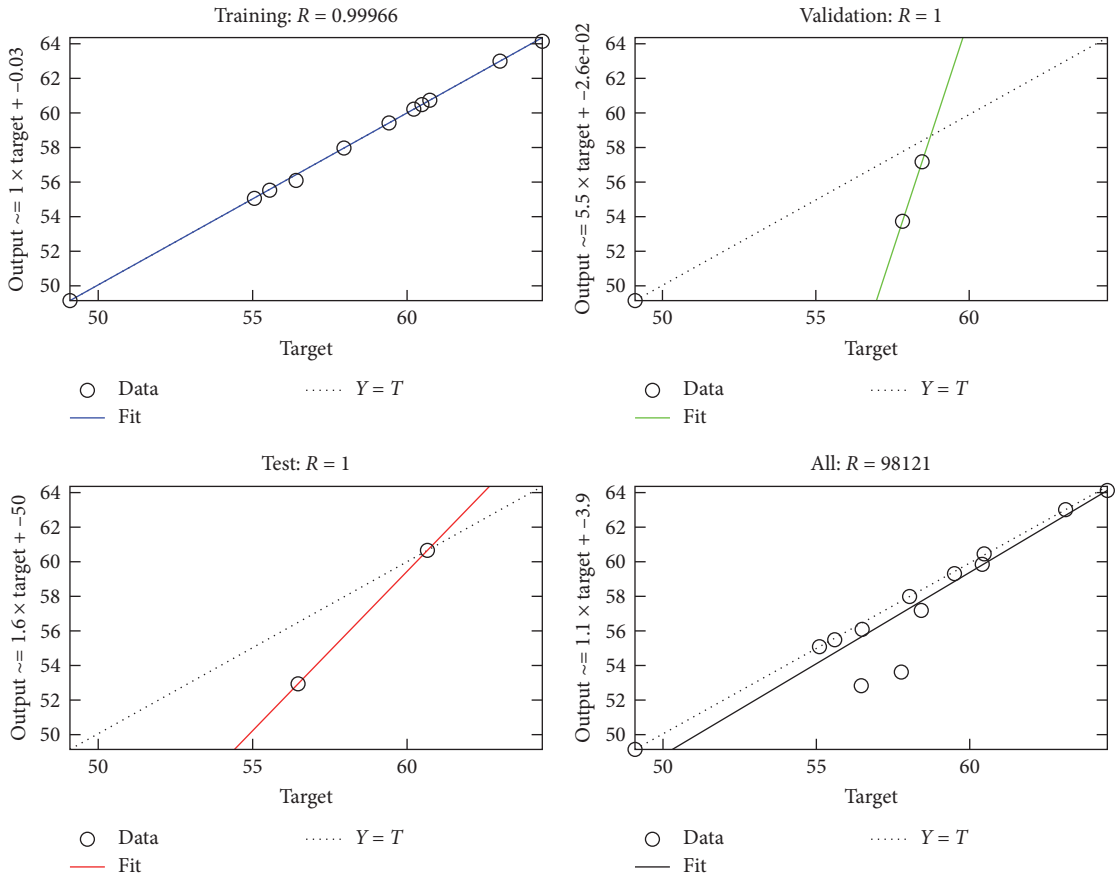

(b)

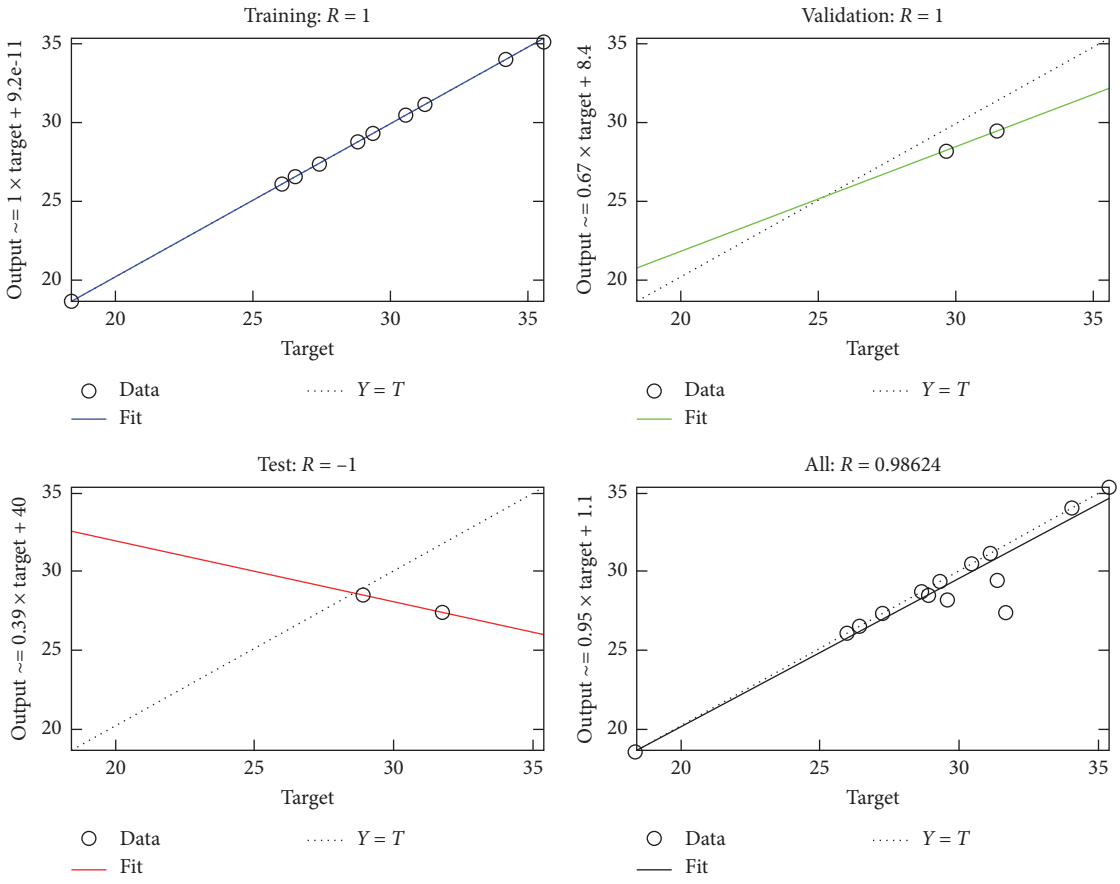

(c)

Figure 7: ANN-predicted results of (a) tensile; (b) flexural; and (c) impact strength of hybrid composites.

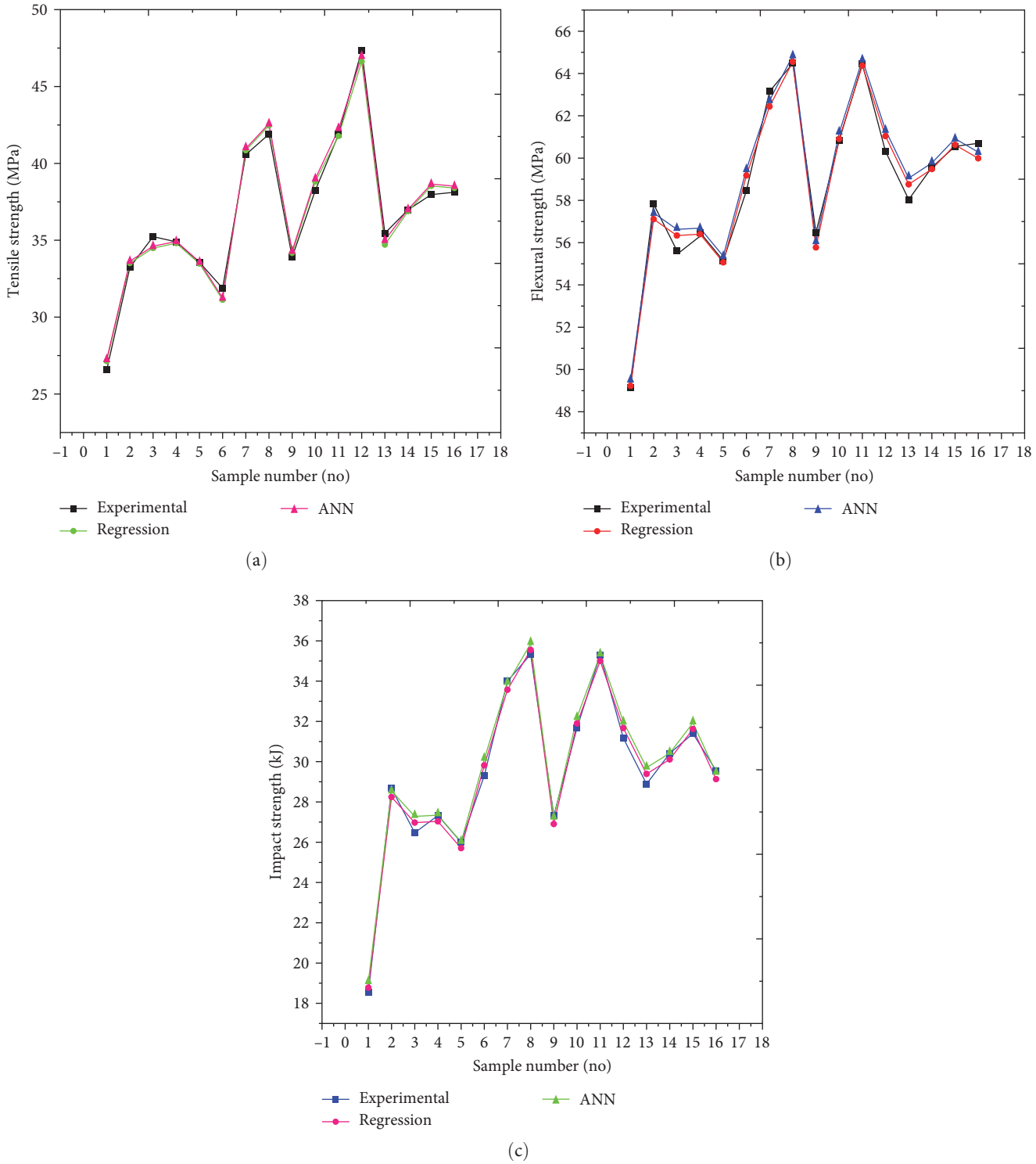

Figure 8: Comparison of experimental vs. regression vs. ANN results of (a) tensile; (b) bending; (c) impact behavior of nanocomposites.

Table 10: Optimum outcomes of nanocomposites.

Response	Factor levels	Experimental	Regression	ANN
Tensile (MPa)	A3, B4, C4, D2	47.36	47.81	47.98
Flexural (MPa)	A3, B4, C4, D2	64.48	65.17	66.28
Impact (kJ)	A3, B4, C4, D2	35.33	35.55	35.86

the study of the data using the conceptual Taguchi's optimization approach, S/N ratio, ANOVA, and regression analysis:

(1) The Taguchi analysis of the present research shows five wt% of nano-SiO_2, 300 gsm of banana fiber mat, 19 MPa of molding pressure, and 110°C of compression molding temperature show the optimum parameters.

(2) The parameters mentioned above exhibit the highest values of mechanical properties, like 47.36 MPa of tensile, 64.48 MPa of flexural, and 35.33 kJ of impact.

(3) Up to 95% accuracy was achieved in predicting the mechanical performance of hybrid nanocomposites using ANN and regression models. Regression and ANN were expected to be more reliable based on the outcome of mechanical properties compared to the actual.

(4) Compared to experimental results, the regression prediction shows 0.94% improvement in tensile, 1.05% in flexural, and 0.61% in impact.

(5) Compared to experimental results, the ANN prediction demonstrates a 1.29% improvement in tensile, 2.71% in flexural, and 1.47% in impact.

(6) As per the ANOVA analysis, the woven banana contributes above 40% to the mechanical strength compared to other parameters because the banana fiber mat acts as a primary stress transmission medium in the current research. It effectively transfers the load to the matrix.

Data Availability

The data used to support the findings of this study are included in the article. Should further data or information be required, these are available from the corresponding author upon request.

Conflicts of Interest

The authors declare that they have no conflicts of interest.

References

[1] T.-T.-L. Doan, H. Brodowsky, and E. Mäder, "Jute fibre/epoxy composites: surface properties and interfacial adhesion," *Composites Science and Technology*, vol. 72, no. 10, pp. 1160–1166, 2012.

[2] N. M. Moustafa, K. A. Mohammed, E. S. Al-Ameen, A. A. F. Ogaili, and M. N. M. Al-Sabbagh, "Mechanical and tribological properties of walnut/polypropylene natural composites," *Journal of Mechanical Engineering Research and Developments*, vol. 43, no. 4, pp. 372–380, 2020.

[3] K. Gunasekaran, R. Annadurai, and P. S. Kumar, "Long term study on compressive and bond strength of coconut shell aggregate concrete," *Construction and Building Materials*, vol. 28, no. 1, pp. 208–215, 2012.

[4] O. Faruk, A. K. Bledzki, H.-P. Fink, and M. Sain, "Biocomposites reinforced with natural fibers: 2000–2010," *Progress in Polymer Science*, vol. 37, no. 11, pp. 1552–1596, 2012.

[5] G. Velmurugan and K. Babu, "Statistical analysis of mechanical properties of wood dust filled jute fiber based hybrid composites under cryogenic atmosphere using grey-Taguchi method," *Materials Research Express*, vol. 7, no. 6, Article ID 065310, 2020.

[6] V. Ganesan and B. Kaliyamoorthy, "Utilization of Taguchi technique to enhance the interlaminar shear strength of wood dust filled woven jute fiber reinforced polyester composites in cryogenic environment," *Journal of Natural Fibers*, vol. 19, no. 6, pp. 1990–2001, 2022.

[7] M. Carus, "The european hemp industry: cultivation, processing and applications for fibres, shives and seeds," n.d., https://www.eiha.org.

[8] R. M. N. Arib, S. M. Sapuan, M. M. H. M. Ahmad, M. T. Paridah, and H. M. D. K. Zaman, "Mechanical properties of pineapple leaf fibre reinforced polypropylene composites," *Materials & Design*, vol. 27, no. 5, pp. 391–396, 2006.

[9] S. Mishra, A. K. Mohanty, L. T. Drzal, M. Misra, and G. Hinrichsen, "A review on pineapple leaf fibers, sisal fibers and their biocomposites," *Macromolecular Materials and Engineering*, vol. 289, no. 11, pp. 955–974, 2004.

[10] M. S. Chowdary, G. Raghavendra, M. S. R. N. Kumar, S. Ojha, and V. Boggarapu, "Influence of nano-silica on enhancing the mechanical properties of sisal/kevlar fiber reinforced polyester hybrid composites," *Silicon*, vol. 14, pp. 539–546, 2022.

[11] G. Velmurugan, V. S. Shankar, S. Kaliappan et al., "Effect of aluminium tetrahydrate nanofiller addition on the mechanical and thermal behaviour of luffa fibre-based polyester composites under cryogenic environment," *Journal of Nanomaterials*, vol. 2022, Article ID 5970534, 10 pages, 2022.

[12] G. Raghavendra, S. Ojha, S. K. Acharya, and S. K. Pal, "Influence of micro/nanofiller alumina on the mechanical behavior of novel hybrid epoxy nanocomposites," *High Performance Polymers*, vol. 27, no. 3, pp. 342–351, 2015.

[13] H. Zhu, Q. Kong, X. Cao, H. He, J. Wang, and Y. He, "Adsorption of Cr(VI) from aqueous solution by chemically modified natural cellulose," *Desalination and Water Treatment*, vol. 57, no. 43, pp. 20368–20376, 2016.

[14] T. Singh, B. Gangil, L. Ranakoti, and A. Joshi, "Effect of silica nanoparticles on physical, mechanical, and wear properties of natural fiber reinforced polymer composites," *Polymer Composites*, vol. 42, no. 5, pp. 2396–2407, 2021.

[15] K. Majeed, M. Jawaid, A. Hassan et al., "Potential materials for food packaging from nanoclay/natural fibres filled hybrid composites," *Materials & Design (1980–2015)*, vol. 46, pp. 391–410, 2013.

[16] G. Jian, Y. Jiao, L. Feng et al., "High energy density of $BaTiO_3$@TiO_2 nanosheet/polymer composites via ping-pong-like electron area scattering and interface engineering," *NPG Asia Materials*, vol. 14, Article ID 4, 2022.

[17] M. Meikandan, M. Karthick, L. Natrayan et al., "Experimental investigation on tribological behaviour of various processes of anodized coated piston for engine application," *Journal of Nanomaterials*, vol. 2022, Article ID 7983390, 8 pages, 2022.

[18] H. A. Sallal, A. A. Abdul-Hamead, and F. M. Othman, "Effect of nano powder (Al_2O_3–CaO) addition on the mechanical properties of the polymer blend matrix composite," *Defence Technology*, vol. 16, no. 2, pp. 425–431, 2020.

[19] K. R. Sumesh and K. Kanthavel, "Synergy of fiber content, Al_2O_3 nanopowder, NaOH treatment and compression

pressure on free vibration and damping behavior of natural hybrid-based epoxy composites," *Polymer Bulletin*, vol. 77, pp. 1581–1604, 2020.

[20] L. Giraldo, D. P. Vargas, and J. C. Moreno-Piraján, "Study of CO_2 adsorption on chemically modified activated carbon with nitric acid and ammonium aqueous," *Frontiers in Chemistry*, vol. 8, Article ID 543452, 2020.

[21] N. Saba, M. T. Paridah, K. Abdan, and N. A. Ibrahim, "Effect of oil palm nano filler on mechanical and morphological properties of kenaf reinforced epoxy composites," *Construction and Building Materials*, vol. 123, pp. 15–26, 2016.

[22] R. A. Ilyas, S. M. Sapuan, M. S. N. Atikah et al., "Effect of hydrolysis time on the morphological, physical, chemical, and thermal behavior of sugar palm nanocrystalline cellulose (*Arenga pinnata (Wurmb.) Merr*)," *Textile Research Journal*, vol. 91, no. 1-2, pp. 152–167, 2021.

[23] M. Barczewski, K. Sałasińska, and J. Szulc, "Application of sunflower husk, hazelnut shell and walnut shell as waste agricultural fillers for epoxy-based composites: a study into mechanical behavior related to structural and rheological properties," *Polymer Testing*, vol. 75, pp. 1–11, 2019.

[24] L. Natrayan and M. S. Kumar, "An integrated artificial neural network and Taguchi approach to optimize the squeeze cast process parameters of AA6061/Al_2O_3/SiC/Gr hybrid composites prepared by novel encapsulation feeding technique," *Materials Today Communications*, vol. 25, Article ID 101586, 2020.

[25] P. Sabarinathan, V. E. Annamalai, K. Vishal et al., "Experimental study on removal of phenol formaldehyde resin coating from the abrasive disc and preparation of abrasive disc for polishing application," *Advances in Materials Science and Engineering*, vol. 2022, Article ID 6123160, 8 pages, 2022.

[26] J. Zhu, Y. Shi, X. Feng, H. Wang, and X. Lu, "Prediction on tribological properties of carbon fiber and TiO_2 synergistic reinforced polytetrafluoroethylene composites with artificial neural networks," *Materials & Design*, vol. 30, no. 4, pp. 1042–1049, 2009.

[27] K. R. Sumesh and K. Kanthavel, "Optimizing various parameters influencing mechanical properties of banana/coir natural fiber composites using grey relational analysis and artificial neural network models," *Journal of Industrial Textiles*, vol. 51, no. 4_suppl, pp. 6705S–6727S, 2022.

[28] N. Sharma, S. Kumar, and K. K. Singh, "Taguchi's DOE and artificial neural network analysis for the prediction of tribological performance of graphene nano-platelets filled glass fiber reinforced epoxy composites under the dry sliding condition," *Tribology International*, vol. 172, Article ID 107580, 2022.

[29] S. Kumar, Priyadarshan, and S. K. Ghosh, "Statistical and artificial neural network technique for prediction of performance in $AlSi_{10}Mg$-MWCNT based composite materials," *Materials Chemistry and Physics*, vol. 273, Article ID 125136, 2021.

[30] Z. Jiang, Z. Zhang, and K. Friedrich, "Prediction on wear properties of polymer composites with artificial neural networks," *Composites Science and Technology*, vol. 67, no. 2, pp. 168–176, 2007.

[31] H. M. Gomes, A. M. Awruch, and P. A. M. Lopes, "Reliability based optimization of laminated composite structures using genetic algorithms and artificial neural networks," *Structural Safety*, vol. 33, no. 3, pp. 186–195, 2011.

[32] P. E. Imoisili and T.-C. Jen, "Modelling and optimization of the impact strength of plantain (*Musa paradisiacal*) fibre/MWCNT hybrid nanocomposite using response surface methodology," *Journal of Materials Research and Technology*, vol. 13, pp. 1946–1954, 2021.

[33] A. S. Kaliappan, S. Mohanamurugan, and P. K. Nagarajan, "Numerical investigation of sinusoidal and trapezoidal piston profiles for an IC engine," *Journal of Applied Fluid Mechanics*, vol. 13, no. 1, pp. 287–298, 2020.

[34] A. Kumar, J. Kumar, and D. Juneja, "Optimization of process parameters and mechanical properties of hybrid fibre reinforced by epoxy resin by response surface methodology (RSM)," *International Journal of Research in Engineering and Innovation*, vol. 3, no. 6, pp. 399–407, 2019.

[35] S. K. Sundaram and S. Jayabal, "Regression modeling and particle swarm optimization of mechanical properties of potassium hydroxide pretreated Dharbai fiber–reinforced polyester composites," *Proceedings of the Institution of Mechanical Engineers, Part L: Journal of Materials: Design and Applications*, vol. 230, no. 1, pp. 105–115, 2016.

[36] H. S. S. Tomo, O. Ujianto, R. Rizal, and Y. Pratama, "Effects of number of ply, compression temperature, pressure and time on mechanical properties of prepreg kenaf–polypropilene composites," *IOP Conference Series: Materials Science and Engineering*, vol. 223, Article ID 012026, 2017.

[37] K. S. H. Kumar and B. Siddeswarappa, "Influence of TiO_2–coconut shell ash hybrid reinforcement on mechanical performance of Al6061 composites," *International Journal of Mechanical Engineering*, vol. 6, pp. 864–873, 2021.

[38] C. J. Schwartz and S. Bahadur, "Studies on the tribological behavior and transfer film–counterface bond strength for polyphenylene sulfide filled with nanoscale alumina particles," *Wear*, vol. 237, no. 2, pp. 261–273, 2000.

[39] J. Datta, P. Kosiorek, and M. Włoch, "Effect of high loading of titanium dioxide particles on the morphology, mechanical and thermo–mechanical properties of the natural rubber–based composites," *Iranian Polymer Journal*, vol. 25, pp. 1021–1035, 2016.

[40] C. Cazan, A. Enesca, and L. Andronic, "Synergic effect of TiO_2 filler on the mechanical properties of polymer nanocomposites," *Polymers*, vol. 13, no. 12, Article ID 2017, 2021.

[41] H. S. Bedi and P. K. Agnihotri, "Effect of carbon nanotubes on the interlaminar and fracture properties of carbon fibre/epoxy composites," *Indian Journal of Engineering and Materials Sciences*, vol. 27, no. 6, pp. 1136–1140, 2020.